Planning station capacity and fleet size of one-way electric carsharing systems with continuous state of charge functions

Huang, Kai; An, Kun; Correia, Gonçalo Homem de Almeida

DOI
10.1016/j.ejor.2020.05.001

Publication date
2020

Document Version
Accepted author manuscript

Published in
European Journal of Operational Research

Citation (APA)
Huang, K., An, K., & Correia, G. H. D. A. (2020). Planning station capacity and fleet size of one-way electric carsharing systems with continuous state of charge functions. *European Journal of Operational Research*, *287*(3), 1075-1091. https://doi.org/10.1016/j.ejor.2020.05.001

Important note
To cite this publication, please use the final published version (if applicable).
Please check the document version above.

Planning Station Capacity and Fleet Size of One-way Electric Carsharing Systems with Continuous State of Charge Functions

Kai Huang[2], Kun An[1]*, Gonçalo Homem de Almeida Correia[3]
[1]College of Transportation Engineering, Tongji University, 4800 Cao'an Road, Shanghai, China
[2]Institute of Transport Studies, Department of Civil Engineering, Monash University, Melbourne, Australia
[3]Department of Transport & Planning, Delft University of Technology, Delft, Nederland
*Email: kunan@tongji.edu.cn

Abstract
This paper presents a method for determining the deployment of one-way electric carsharing services within a designated region that maximizes the total profit of the operator. A mixed integer non-linear program model is built, with a strategic planning level that decides the fleet size and the station capacity and an operational level that decides on the required relocation operations. The state of charge (SOC) of the vehicles parked in one station is assumed to follow a continuous distribution. A rolling horizon method is used to optimize the operational decisions over the course of a day, considering demand fluctuations and the limited battery capacity of the vehicles. A golden section line search method and a shadow price algorithm are developed to optimize the fleet size and station capacity, with the results feeding back to the carsharing operations. To demonstrate the applicability of the formulated models and solution algorithms, a large-scale case study is conducted for Suzhou Industrial Park, China as the region of operation. A two-step verification method that combines an optimization model via tracking of individual vehicle SOC and a discrete event simulation, demonstrates the accuracy of the SOC distribution model. Managerial insights from the application are also presented.

Keywords: Transportation; Carsharing; Electric vehicles; Station capacity; Fleet size; Relocations

1 Introduction

One-way carsharing allows users to return vehicles to any designated parking station, which may be different from the initial pick-up station (Shaheen et al., 2015). Compared to the round-trip carsharing system in which vehicles are returned to the original parking station, one-way carsharing has the apparent advantages of encouraging the use of carsharing services and making the carsharing system more competitive (Jorge et al., 2015; Yoon et al., 2017; Huang et al. 2018). Because of the significant added convenience, one-way carsharing is attracting a growing number of users (Nair and Miller-Hooks, 2014), and many start-ups, as well as traditional car rental companies, have begun to offer one-way carsharing services, e.g., Zipcar, Hertz, GoGet, Go4carrental, and EVCARD. The rapid growth of carsharing companies across the world is unlocking the potential of the sharing economy in the mobility sector.

There is a growing trend of providing carsharing services using Electric Vehicles (EVs) because of the environmental benefits involved. EVs contribute to reducing local air pollution, and if aligned with clean energy practices, can contribute significantly to reductions in greenhouse gas emissions (Yang et al., 2016). According to a stated preference survey conducted in Korea, it is believed that CO_2 emissions could be reduced to as much as 655,773 t per year if the number of EV charging stations reaches 50% of the current number of Internal Combustion Engine Vehicles (ICEV) fuel stations (Jung and Koo, 2018). Therefore, one-way electric carsharing offers significant environmental benefits compared with its internal combustion engine counterpart. However, it presents significantly greater challenges for both operational decision-making and strategic planning for carsharing systems owing to station-based demand-supply imbalances and the limited battery capacity of EVs (Firnkorn and Müller, 2015; Lu et al., 2018; Zhang et al., 2019).

At the operational level, one notable difficulty arises from intrinsic asymmetry and fluctuations in demand. To deal with the imbalance between demand and the available vehicles at different stations, operators implement vehicle relocations that transport vehicles from surplus zones to deficit zones (Bruglieri et al., 2017; Jorge et al., 2014; Wang et al., 2019). Drivers are needed to relocate vehicles, and this comes at a significant cost for the operators. To maximize total profit, operators need to weigh relocation costs against carsharing revenues. In the literature, Mixed Integer Programming (MIP) has been used to manage fleet redistribution when demand is known either through forecasting or based on historical data (Kek et al., 2009; Huang et al. 2018).

Employing EVs further adds to the difficulty of managing these relocations as the state of charge (SOC) of each vehicle needs to be tracked to ensure that the remaining battery capacity is sufficient for the upcoming carsharing demand or relocations. Given the scale of carsharing fleet sizes, modeling the SOC of each vehicle every minute of the day would require an enormous number of integer variables (Correia and Santos, 2014). Zhao et al. (2018) studied the EV rebalancing and staff relocation problem by tracking the SOC of each vehicle in a carsharing system of up to 130 vehicles and 60 drivers. It is a formidable task to solve such a large-scale MIP regarding vehicle relocations, idle time for charging, and passenger/vehicle movements. Consequently, it is natural for researchers to explore model simplification or heuristic techniques as alternatives (Jorge et al., 2012).

One stream of studies on EV sharing relocation adopts simplified charging strategies to formulate a trackable EV relocation problem (Liang et al. 2016). For example, EVs are only made available for rent or are relocated when they are charged to a certain capacity, i.e., the SOC equals a predefined value (Li et al., 2016; Brandstätter et al., 2017; Xu et al., 2018). Once a vehicle arrives at a parking station, it is required to remain there for a predetermined period to be recharged. Xu et al. (2018) formulated a concise non-linear program for EV relocations assuming that vehicles must be fully recharged before each departure. Thus, it would be unnecessary to record the SOC, with vehicles marked as unavailable for the period of recharging after each trip. This considerably reduces the model scale. However, it is

unrealistic and uneconomical to fully charge the vehicles during rush hour when there is a great demand for carsharing (Boyacı et al., 2017).

Another stream of studies on EV sharing and relocation captures the changing SOC of vehicles through time-space network constraints or via simulation-based methods. Gambella et al. (2018) established a space-time network model to address vehicle and personnel movements in an electric carsharing system. Zhang et al. (2019) built another space-time network flow model for tracking vehicle SOC in a different dimension that listed the number of vehicles with different battery states rather than specifying the SOC of each vehicle. However, in a large network, the Zhang et al. (2019) model faces a computation burden problem. Alternatively, simulation-based methods can be used to evaluate different charging strategies for a large network, but they overlook whole system optimization (Scheltes and Correia, 2017).

Strategic/tactical planning of carsharing systems aims to investigate long-term resource deployment, e.g., exclusive charging/parking stations and their corresponding capacity and EV fleet size, which is crucial for guaranteeing financial sustainability. Strategic planning for carsharing systems is significantly impacted by operational level decisions, including relocation schemes and charging schedules (Li et al., 2016). Correia and Antunes (2012) pointed out the importance of station location and vehicle relocations in response to the demand-supply imbalance problem. Strategic decisions should be optimized considering the impact of operational decisions that will be made subsequently (Cepolina and Farina, 2012; Fassi et al., 2012; Jorge et al., 2012). However, all these vehicle relocation methods present significant challenges to the carsharing operator when engaging in strategic planning for a large-scale electric carsharing system.

There are only a few of studies on the strategic planning problem for electric carsharing systems. Xu et al. (2018) established an optimization model for determining the EV fleet size by considering vehicle and personnel movements. Furthermore, to avoid requiring the vehicles to be fully charged before departures, Boyacı et al. (2017) proposed an integrated optimization in which recharging requirements were addressed via a simulation module. Existing studies typically assume that each parking space is equipped with a charger (e.g., Xu et al., 2018), which matches the current practices of operators such as EVCARD. A charging pile in every parking space ensures that all parked vehicles can be recharged. Hu and Liu (2016) optimized the station capacity and fleet size in a queuing network, considering road congestion, booking time windows, and parking space utilization constraints. Hua et al. (2019) jointly optimized station location and fleet management under demand uncertainty via a multi-stage spatial-temporal network. However, the aforementioned research either intentionally scaled down the EV fleet to maintain the tractability of the problem, or encountered major challenges for the carsharing operator when engaging in strategic planning for a large-scale electric carsharing system.

This study fills this gap by encapsulating the time-varying SOC of EVs into the optimization of strategic planning for real-world electric carsharing systems while considering the impact of operational level decisions. As mentioned earlier, requiring vehicles to fully recharge before departure reduces their utilization rate, while tracking the SOC of each vehicle incurs a heavy computation burden. Alternatively, we assume that the SOC of vehicles parked in a station follows a continuous distribution, with its parameters changing over time. A recursive equation is developed to calculate the average SOC of the vehicles in a station at any time step, based on which a mixed integer non-linear program (MINLP) is formulated.

To handle the computation burden, we split the large-scale MINLP into two subproblems: one to obtain the fleet size and station capacity at the strategic level, and the other to obtain vehicle relocations at the operational level. Jointly optimizing the two levels is necessary owing to the feedback loop between both levels. Allocating only a few vehicles or renting only a few parking spaces for a large demand will lead to several unsatisfied requests, whereas if many vehicles and parking spaces are allocated, the

system may be underused. Studying an integrated problem while considering strategic planning and operational decisions simultaneously has become an important challenge (Hu and Liu, 2016; Deng and Cardin, 2018). At the strategic level, we first obtain the upper bound and lower bound of the fleet size by assuming fully charged EVs before departure or using EVs without battery capacity constraints, respectively. Given the fleet size and station capacity, a series of small-scale linear programs (LPs) is built to determine vehicle relocations for fulfilling travel demand in a rolling horizon framework. A shadow price algorithm and a golden section line search method are further developed to optimize the station capacity and fleet size such that the total profit can be maximized.

The remainder of this paper is organized as follows: In Section 2, the station-based one-way electric carsharing mathematical model is established. In Section 3, the solution algorithms are proposed. Section 4 presents a case study conducted in Suzhou Industrial Park (SIP), China. Section 5 provides some concluding remarks on the algorithms and their application in the case study.

2 Model formulation

2.1 Assumptions

The assumptions used in this study are as follows:

- The distribution of travel demand and travel time is time-varying over the course of a day;
- The travel demand in a typical workday is utilized in making strategic planning decisions, while demand uncertainty or changes in demand from day to day is not considered;
- Every carsharing parking space has a charging pile;
- The SOC of vehicles parked at a station at a time instant obeys a continuous distribution whose mean changes over time;
- When two vehicles are used to service two trips, the one with the larger SOC is used to service the longer trip.

2.2 Problem setting

The operator aims to maximize profit by optimizing the fleet size and station capacity of a station-based one-way carsharing system for a predefined region. In operation management, demand satisfaction and vehicle relocations are considered simultaneously, which provides feedback for the strategic planning problem. Fleet size, station capacity, demand satisfaction, and vehicle relocations are decision variables. A typical workday's demand, which is a given parameter, is utilized in the long-term strategic planning and the capital costs, including vehicle costs and station opening costs, are expressed as depreciation costs per day. It is possible that not all requests are satisfied. EVs are used to provide the service, and the SOC of vehicles parked in a station is assumed to follow a continuous distribution model, which can be seen as auxiliary decision variables. Vehicles with higher SOCs are used to service longer trips. We consider a scenario where customers make reservations in advance and the operator can assign vehicles to customers.

The studied region is divided into $|I|$ traffic zones where index i or j denotes one traffic zone. Parked vehicles and allocated parking spaces can only be used to service the travel demand occurring in their own traffic zone. A day of operation is divided into $|T|$ time steps, where $t \in T$ denotes a time step. Client trips and vehicle relocations occur at the beginning of a time step. Let q_{ijt} denote the carsharing demand to move from traffic zone i to traffic zone j, where $i \neq j$, at time step t. Only the trips between two zones are considered. The company purchases a certain number of EVs V_{sum} and rents a number of parking spaces S_i in zone i, all with chargers installed, to ensure that returned vehicles can be charged immediately. During operation, the demand-supply imbalance problem is handled using

relocation operations. Based on the predicted travel demand, the operator relocates N_{ijt} vehicles from traffic zone i to traffic zone j at time instant t to fulfill the future demand. Because the number of travelers serviced by carsharing, i.e., Q_{ijt}, is impacted by the available vehicles in traffic zone i at time instant t, we impose a penalty of c_p for each unsatisfied trip. The penalty can be seen as an allowance with which unserved clients can purchase a public transport ticket. This helps to prevent customer loss over the long term and makes carsharing unsustainable. If profit maximization, regardless of the demand fulfillment rate, is the goal of the operator, one can simply set $c_p = 0$. Table 1 presents a complete notation list.

Table 1 Notation list

Parameters	
c_0	Rental price of a shared EV per time step
c_e	Electricity consumption costs per time step
c_f	Fixed costs per vehicle per day, including depreciation costs and maintenance costs
c_p	Penalty for rejecting a single trip
c_r	Costs of relocating an EV per time step
c_s	Rental costs of a parking space per day
$I:\{i\}$	Set of traffic zones into which an urban area is divided
$T:\{t\}$	Set of time steps, where t is also used to denote the beginning of time step t
K	Number of time steps in one horizon of the rolling horizon framework
g_{ijt}	Travel time in time steps from zone $i \in I$ to zone $j \in I$, where $i \neq j$ departing at the beginning of time step $t \in T$
q_{ijt}	Travel demand from traffic zone i to traffic zone j, where $i \neq j$ at time step t
ij_r	An origin and destination (OD) pair from zone i to zone j_r, where j_r is the index of the destination zone at the r^{th} ascending order in travel time among all origins and destinations starting from zone i, and $r \in 1,...,\lvert I \rvert - 1$
s_i	Maximum number of parking spaces in zone i
α	Recharging speed: as SOC increase (%) per time step
β	Discharging speed: as SOC decrease (%) when a vehicle drives for one time step
ζ	Weight for the future profits in the rolling horizon framework
Decision variables	
S_i	Number of parking spaces in zone i
V_{it}	Number of shared EVs in zone i at time instant t
V_{sum}	Fleet size of the carsharing system
N_{ijt}	Number of relocated vehicles from traffic zone i to traffic zone j, where $i \neq j$ at time instant t
Q_{ijt}	Satisfied travel demand to move from traffic zone i to traffic zone j, where $i \neq j$ at time instant t
Auxiliary variables	
E_{it}	A random variable that represents the SOC of vehicles parked in zone i at time instant t

$p_{ij_r t}$	Proportion of vehicles from zone i to zone j_r at time instant t
P_{irt}	Cumulative probability of vehicles heading to destinations closer than and equal to the r^{th} destination from zone i at time instant t
V_{sum}	Fleet size of purchased vehicles, with $V_{sum} = \sum_{i \in I} V_{i1}$
W_{it}	Number of idle vehicles in traffic zone i at time step t
$\eta_{ij_r t}$	Average SOC of vehicles that head to destination j_r from zone i at time step t, including client trips and relocations
μ_{it}	Average SOC of all the vehicles parked in traffic zone i at time instant t
π_{it}	Shadow price related to the parking space constraint in traffic zone i at time step t
Functions	
$f(x)$	Probability density function of the continuous SOC distribution
$F(x)$	Cumulative distribution function of the continuous SOC distribution
$G(x,u)$	Recharging function, where x is the current SOC and u is recharging time
$H(x,u)$	Discharging function, where x is the current SOC and u is discharging time

2.3 Mathematical model

2.3.1 Continuous SOC distribution

To facilitate formulation of the model, a series equation is constructed to capture vehicle SOC changes. Due to the battery capacity constraint of EVs, not all parked vehicles can be used by carsharing users. Only those with enough battery capacity to cover the upcoming trip can be rented or relocated. It is necessary to identify the vehicles that are able to embark on the desired trips based on the SOC of the parked vehicle. Thus, we construct a continuous SOC distribution model to simulate the SOC changes over time, as detailed in the next section.

Let E_{it} be a random variable that represents the SOC of vehicles parked in zone i at time instant t. We assume that E_{it} follows a continuous distribution $E_{it} \sim D\left(\mu_{it}, \sigma^2\left(\mu_{it}\right)\right)$, with mean μ_{it} and variance σ^2. The probability density function (PDF) is $f_{E_{it}}\left(x\right)$, and the cumulative distribution function (CDF) is denoted by $F_{E_{it}}\left(x\right) = \int_{-\infty}^{x} f_{E_{it}}\left(\omega\right) d\omega$. Because the SOC of a vehicle is in the range [0,1], i.e., $0 \le E_{it} \le 1$ (between 0% and 100% of the total battery power), the variance σ^2 should be properly defined, such that the majority of the E_{it} values fall within the range of [0,1].

Thus, instead of tracking the SOC of each vehicle, only the average SOC μ_{it} in zone i at time instant t needs to be tracked. We hypothesize that the proposed continuous SOC distribution model can significantly reduce the number of variables while capturing their time-varying property. The assumption of a continuous SOC distribution is verified in the case study (Section 4.4).

In operation, once a vehicle arrives at a station, it is recharged, with its SOC increasing according to the linear recharging function expressed in Eq. (1). When a vehicle is rented or relocated, the initial SOC reduces gradually with travel time, according to the linear discharging function in Eq. (2). Let us assume that the SOC of a vehicle arriving in traffic zone i at time instant t is x. In Eq. (1), α is the battery recharging speed in percentage (%) per time step, and the percentage of battery capacity recharged in one time step is assumed to be equal at all charging stations. $G(x,u)$ calculates the vehicle SOC after being recharged for a time duration of u; this SOC cannot exceed the maximum level of 100%. In Eq. (2), β is the battery consumption speed in % per time step, with the percentage of battery capacity

consumed after driving for one time step assumed to be equal for all vehicles across the fleet. $H(x,u)$ calculates the vehicle SOC after servicing a trip with a travel time of u. To ensure that $H(x,u)$ is positive, the travel time u cannot exceed the driving range of the vehicle.

$$G(x,u) = \min\{x + \alpha u, 1\} \tag{1}$$

$$H(x,u) = x - \beta u \tag{2}$$

When relocating a vehicle or renting a vehicle to a client, it must be ensured that the vehicle SOC is sufficient to complete the trip. For simplicity of the model formulation, we use a simple rule of customer-vehicle assignment: vehicles with larger SOC are used to service longer trips. The effects of other customer-vehicle assignment schemes on the profitability of the carsharing system, including first come first serve or random assignment, will be left to future studies. We first rank the trips starting from zone i at time instant t in ascending order of the travel time g_{ijt}. Then, let j_r be the destination zone with the r^{th} smallest travel time, where $r = 1,2,...,|I|-1$. Thus, we have $Q_{ij_r t}$ and $N_{ij_r t}$ denoting satisfied demand and vehicles relocated from zone i to zone j_r, respectively, at time instant t.

$$Q_{ij_r t} + N_{ij_r t} \le V_{it}\left(1 - F_{E_{it}}\left(\beta g_{ij_r t}\right)\right) - \sum_{n=r+1}^{|I|-1}\left(Q_{ij_n t} + N_{ij_n t}\right) \quad \forall i \in I,\ r \in 1,...,|I|-1,\ t \in T \tag{3}$$

Eq. (3) specifies the vehicle SOC constraints. $Q_{ij_r t} + N_{ij_r t}$ on the left denotes the number of trips from zone i to zone j_r at t. The minimum SOC required to makes these trips is $\beta g_{ij_r t}$, i.e., the product of the travel time and the discharge speed. Based on the SOC distribution of vehicles parked in zone i, $V_{it}\left(1 - F_{E_{it}}\left(\beta g_{ij_r t}\right)\right)$ calculates the number of vehicles with an SOC larger than $\beta g_{ij_r t}$ available to realize trips from zone i to zone j_r at t. Among the vehicles with SOC greater than $\beta g_{ij_r t}$, some could be used to service longer trips with a destination rank higher than r. Vehicles already assigned to the other travel time ranks are given by $\sum_{n=r+1}^{|I|-1}\left(Q_{ij_n t} + N_{ij_n t}\right)$. Eq. (3) states that trips made from zone i to zone j_r at t cannot exceed the available vehicles, with sufficient SOC, parked at zone i. Notably, Eq. (3) does not require long trips to be prioritized. Thus, it is possible that a request with a short travel time is fulfilled, $Q_{ij_r t} > 0$, and a long trip is not, $Q_{ij_n t} = 0, n > r$, while the vehicles actually have enough battery capacity to service both. The demand selection is simply a result of the optimization. We only assume that if trips A and B are both satisfied, with the travel time of A being longer, then the vehicle with higher SOC is used for trip A.

At the beginning of the day, all vehicles are fully charged, with $\mu_{i1} = 1$. In zone i at time instant t, the available vehicles V_{it} have three options: servicing passenger demand, being relocated, or staying to be charged. Eq. (4) represents this conservation at instant t, where W_{it} is the number of idle vehicles for the entire time step. Given that long trips use vehicles with a large SOC, the available vehicles parked in zone i at time instant t can be divided into $|I|$ portions, each assigned with a probability of $p_{ij_r t}$ (see Fig. 1), where $p_{ij_r t}, r = 1,...|I|-1$ is the proportion of vehicles heading to destination j_r at time t and p_{iit} is the proportion of idle vehicles. These calculations are given by Eqs. (5) and (6). The

cumulative probability P_{irt} of vehicles from zone i heading to destinations closer than and equal to the r^{th} destination at t is given by Eq. (7). According to the SOC CDF function, the corresponding quantile value $F^{-1}(P_{irt})$ provides the boundary value of the SOC required to support these trips. The vehicles heading to destination j_r have SOC values ranging from $F^{-1}(P_{i,r-1,t})$ to $F^{-1}(P_{irt})$ (horizontal axis in Fig. 1). We use $\eta_{ij_rt}, r=1,...|I|-1$ to denote the average SOC of vehicles heading to destination j_r, and η_{iit} to indicate the average SOC of idle vehicles. Eqs. (8) and (9) present the calculation as the integral of the scaled-up density function in the range $F^{-1}(P_{i,r-1,t})$ to $F^{-1}(P_{irt})$.

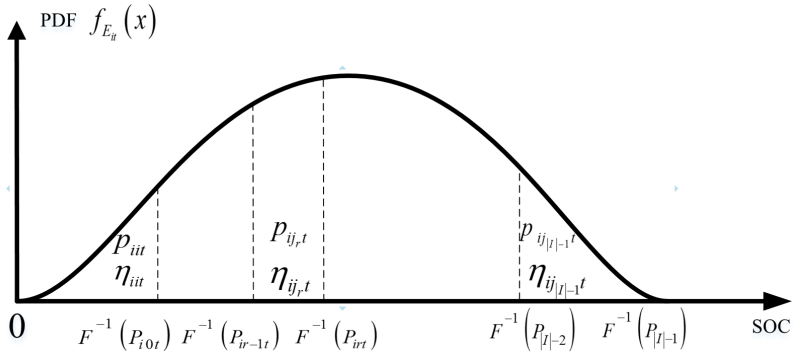

Fig. 1 PDF of the SOC of vehicles at station i at time instant t

$$V_{it} = W_{it} + \sum_{r=1}^{|I|-1}\left(Q_{ij_rt} + N_{ij_rt}\right) \quad \forall i \in I,\ t \in T \tag{4}$$

$$p_{ij_rt} = \frac{Q_{ij_rt} + N_{ij_rt}}{V_{it}} \quad \forall i \in I, t \in T,\ r = 1,...,|I|-1 \tag{5}$$

$$p_{iit} = \frac{W_{it}}{V_{it}} \quad \forall i \in I,\ t \in T \tag{6}$$

$$P_{irt} = \sum_{n=0}^{r} p_{ij_nt} \quad \forall i \in I, t \in T,\ r = 0,1,...,|I|-1 \tag{7}$$

$$\eta_{ij_rt} = \int_{F^{-1}(P_{ir-1t})}^{F^{-1}(P_{irt})} \frac{f_{E_{it}}(x)}{p_{ij_rt}} x dx \quad \forall i \in I,\ t \in T, r = 1,...,|I|-1 \tag{8}$$

$$\eta_{iit} = \int_{0}^{F^{-1}(P_{i0t})} \frac{f_{E_{it}}(x)}{p_{iit}} x dx \quad \forall i \in I,\ t \in T \tag{9}$$

$$\mu_{it+1} = \frac{G(\eta_{iit},1)W_{it} + \sum_{j \in I} G(H(\eta_{jim}, g_{jim}), \lceil g_{jim} \rceil - g_{jim})\left(Q_{jim} + N_{jim}\right)}{V_{it+1}}$$
$$\forall i \in I,\ t = 1,2,...|T|-1,\ m = max\left\{0, t+1-\lceil g_{jim} \rceil\right\} \tag{10}$$

Next, we formulate a recursive function for the average SOC μ_{it+1} in traffic zone i at time instant $t+1$. At the beginning of the day, we assume all vehicles to be fully charged, i.e., μ_{i1}=1. Eq. (10) calculates the average SOC μ_{it+1} at time instant $t+1$, based on the following: vehicles idling at station i at time step t with charging for one full time step; vehicles arriving at station i between time instants t and $t+1$, with battery capacity consumed during the trip and recharging on arrival; total number of vehicles parked in station i at the beginning of time step $t+1$. The recharging and discharging functions are

expressed as Eqs. (1) and (2), respectively. Eq. (1) represents the charging function $G(x,u)$, which calculates the vehicle SOC after it has been recharged and ensures that the vehicle is not overcharged. Taking $G(\eta_{iit},1)$ in Eq. (10) as an example, it can be written as $G(\eta_{iit},1)=\min\{\eta_{iit}+\alpha,1\}$, in the form of Eq. (1). In Eq. (10), $G(\eta_{iit},1)W_{it}$ denotes the total SOC of vehicles parked in traffic zone i after recharging for one time step. $H(\eta_{jim},g_{jim})$ is the remaining SOC of the vehicles after driving for g_{jim} time steps. m is the departure time of the vehicles that arrive at traffic zone i between time instants t and $t+1$. $\lceil g_{jim} \rceil$ denotes the rounding-up travel time. Before the next movement of the returned vehicle, it is recharged for a duration of $\lceil g_{jim} \rceil - g_{jim}$. $\sum_{j\in J} G\left(H\left(\eta_{jim},g_{jim}\right),\lceil g_{jim} \rceil - g_{jim}\right)\left(Q_{jim}+N_{jim}\right)$ represents the total SOC of the vehicles arriving at traffic zone i between time instants t and $t+1$ after being recharged for a parking time $\lceil g_{jim} \rceil - g_{jim}$.

Proposition 1. *The continuous SOC distribution model guarantees electricity conservation in the carsharing system. Vehicle charging has led to equivalent battery capacity increases and vehicle operation has incurred an equivalent battery capacity decrease.*
Proof. See Appendix.

Lemma 1. The average SOC μ_{it} of the vehicles at any time instant t is in the range of [0,1].

Proof. See Appendix.

2.3.2 Mixed Integer Non-linear Program for EV carsharing network design
With vehicle SOC constraints (1)–(10), it is possible to formulate the EV carsharing network design problem.

$$\mathbf{P1}\ \max_{\mathbf{S,V,Q,N}} \phi = \sum_{t\in T}\sum_{i\in I}\sum_{j\in I}\left(c_0-c_e\right)Q_{ijt}g_{ijt} - \sum_{i\in I}c_sS_i - \sum_{i\in I}c_fV_{i1} - \sum_{t\in T}\sum_{i\in I}\sum_{j\in I}c_rN_{ijt}g_{ijt} - \sum_{t\in T}\sum_{i\in I}\sum_{j\in I}c_p\left(q_{ijt}-Q_{ijt}\right) \quad (11)$$

Subject to:

Constraints (1)–(10), plus

$$\mu_{i1}=1 \quad \forall i\in I \quad (12)$$

$$V_{it}\le S_i \quad \forall i\in I,\ t\in T \quad (13)$$

$$S_i\le s_i \quad \forall i\in I,\ t\in T \quad (14)$$

$$Q_{ijt}\le q_{ijt} \quad \forall i\in I,\ j\in I,\ t\in T \quad (15)$$

$$V_{it}\ge\sum_{j\in I}\left(Q_{ijt}+N_{ijt}\right) \quad \forall i\in I,\ t\in T \quad (16)$$

$$\begin{aligned} &V_{it+1}=V_{it}-\sum_{j\in I}\left(Q_{ijt}+N_{ijt}\right)+\sum_{j\in I}\left(Q_{jim}+N_{jim}\right)\\ &\forall i\in I,\ t=1,2,...|T|-1,\ m=max\left\{0,t+1-\lceil g_{jim} \rceil\right\} \end{aligned} \quad (17)$$

$$N_{ijt},Q_{ijt},S_i,V_{it}\in Z^0,\ \forall i\in I,\ j\in I,\ t\in T \quad (18)$$

The objective function (11) maximizes total profit for a carsharing operator, and is equal to carsharing users' travel fees minus the operation costs, which include electricity consumption costs, parking space rental costs, vehicle fixed costs, relocation operation costs and penalty costs for rejected trips. Relocation costs include two components: energy costs and labor costs. Personnel movements are not considered. Constraints (12) define the initial value of the SOC in traffic zone i at the beginning of a

day. All vehicles are fully charged after a night. Constraints (13) require the parking spaces to be enough for the vehicles that have arrived. Constraints (14) impose that the number of parking spaces should not be greater than the upper bound. Constraints (15) state that the satisfied demand Q_{ijt} has to be lower than the total demand q_{ijt} for carsharing. As mentioned earlier, we penalize the rejected trips in to increase the demand satisfaction rate. Constraints (16) ensure that the number of available vehicles is greater than the total satisfied demand Q_{ijt} (one person per vehicle) and the number of relocated vehicles N_{ijt} leaving this station. Constraints (17) calculate the number of vehicles in traffic zone i at time instant $t+1$, and are equal to the available vehicles in traffic zone i at time instant t, minus the vehicle outflow (passenger renting or relocated vehicles) in zone i at time instant t, plus the vehicle inflow arriving in traffic zone i during time step t. Constraints (18) specify the domain of the decision variables.

MINLP **P1** is compact in the number of variables via modeling vehicle flows instead of individual vehicles. However, the difficult integral Constraints (8)–(9) render **P1** impossible to solve using state-of-the-art solvers such as Gurobi, CPLEX, or Xpress, and thus requires an efficient algorithm.

3 Solution algorithm

To handle the computation difficulties, we propose a customized solution algorithm that separates the strategic and operational decisions. In the solution approach: (1) first, we construct a lower bound and an upper bound to the strategic decisions (fleet size and station capacity); (2) For a given fleet size and station capacity, we solve the operational level problem, which sorts the satisfied travel demand, decides vehicle relocation operations, and obtains the corresponding total profit; (3) The optimized fleet size and station capacity are explored in the identified feasible range using the golden section algorithm and shadow price algorithm, respectively, until the total profit cannot be further improved. The shadow price parameter used in Step 3 is obtained from Step 2 by optimizing the operational decisions. The profit for any given fleet size and station capacity in Step 3 is obtained by solving the problem in Step 2. Consequently, the strategic and operational decisions are interrelated with each other in this loop solution approach. The proposed solution algorithm is a hybrid heuristic method, and the term optimization models and optimized results are used throughout this study to contrast with the simulation-based methods. Fig. 2 illustrates the optimization procedure.

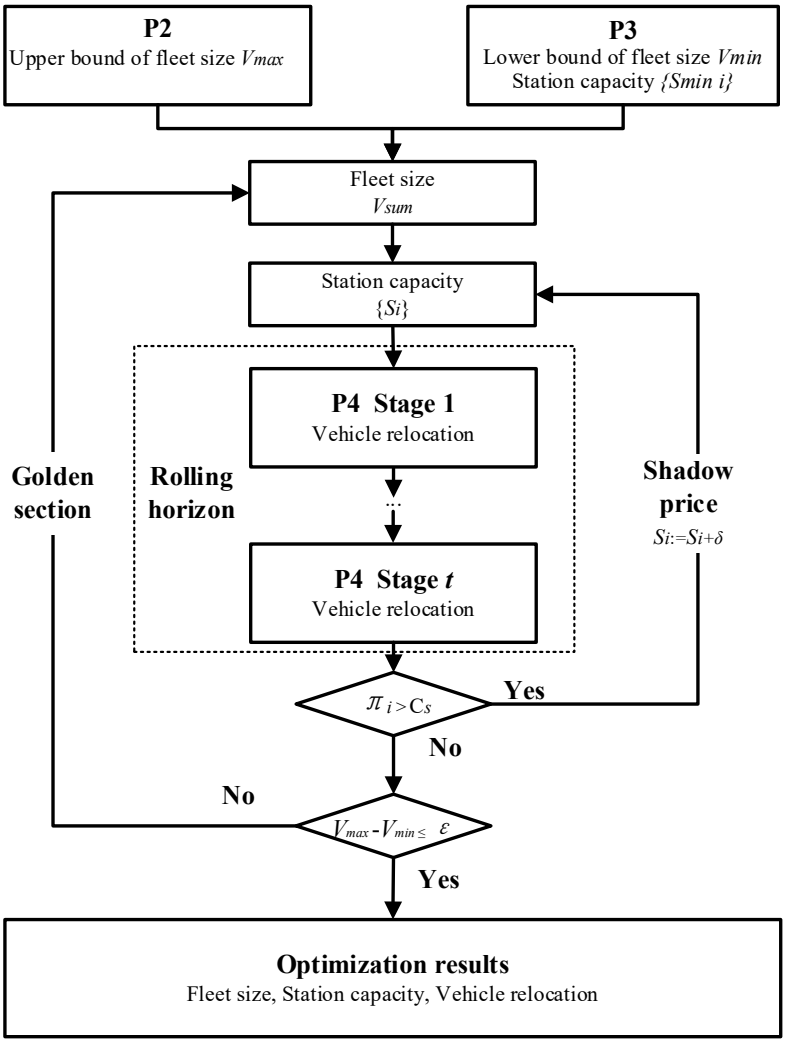

Fig. 2 Flow chart of the solution algorithm

3.1 Strategic level decisions

The strategic decisions in **P1** include the fleet size V_{sum} and station capacity $\{S_i\}$. This section aims to construct an upper bound and a lower bound to fleet size: V_{max} and V_{min}, respectively, and to construct a feasible solution to station capacity.

1) Fleet size upper bound V_{max}

Two constraints are added to derive the fleet size upper bound of **P1**: (a) all travel demand should be satisfied ($Q_{ijt} = q_{ijt}$), and (b) vehicles must be fully charged after each trip before being rented or relocated. Consequently, the SOC related Constraints (1)–(10) can be removed. The rest of the problem can be formulated as the following mixed integer linear program (MILP)

P2
$$\max_{\mathbf{S,V,N}} \phi_{lb} = \sum_{t\in T}\sum_{i\in I}\sum_{j\in I}(c_0 - c_e)q_{ijt}g_{ijt} - \sum_{i\in I}c_s S_i - \sum_{i\in I}c_f V_{i1} - \sum_{t\in T}\sum_{i\in I}\sum_{j\in I}c_r N_{ijt}g_{ijt} \tag{19}$$

Subject to:

Constraints (14), plus

$$V_{it} \geq \sum_{j\in I}\left(q_{ijt} + N_{ijt}\right) \quad \forall i \in I,\ t \in T \tag{20}$$

$$V_{it} + \sum_{m \in M} \sum_{j \in I} \left(q_{jim} + N_{jim} \right) \le S_i \quad \forall i \in I, t \in T$$
$$\text{where } M := \left\{ m \middle| m + g_{jim} \le t; m + g_{jim} \left(1 + \frac{\beta}{\alpha} \right) > t \right\} \tag{21}$$

$$V_{it+1} = V_{it} - \sum_{j \in I} \left(q_{ijt} + N_{ijt} \right) + \sum_{m \in M} \sum_{j \in I} \left(q_{jim} + N_{jim} \right) \quad \forall i \in I, \ t = 1, 2, ... |T| - 1$$
$$\text{where } M := \left\{ m \middle| t < m + g_{jim} \left(1 + \frac{\beta}{\alpha} \right) < t + 1 \right\} \tag{22}$$

$$N_{ijt}, S_i, V_{it} \ge 0, \text{ integer}, \quad \forall i \in I, j \in I, t \in T \tag{23}$$

The objective function (19) maximizes total profit of the operator. Here, V_{it} denotes the number of vehicles with full battery capacity (SOC = 100%) in traffic zone i at time instant t. Consequently, V_{it} are vehicles available for use by clients because vehicles must be fully charged before departure. Constraints (20) ensure that the number of available vehicles is larger than the total demand q_{ijt} and vehicle relocations N_{ijt} leaving a particular station. Constraints (21) are the parking capacity constraints. The parked vehicles in traffic zone i at time instant t include those fully recharged, V_{it}, as well as those that need charging, $\sum_{j \in I} \left(q_{jim} + N_{jim} \right)$. The set $M = \{m\}$ derives the departure times of vehicles that have arrived in zone i before time instant t, $m + g_{jim} \le t$, and those that have not been fully charged at time instant t, $m + g_{jim} \left(1 + \beta / \alpha \right) > t$. Constraints (22) calculate the number of available vehicles with full SOC in traffic zone i at time instant $t+1$, and is equal to the available vehicles V_{it} minus the vehicles going out $\sum_{j \in I} \left(q_{ijt} + N_{ijt} \right)$, plus the vehicles arriving in traffic zone i in time step t $\sum_{j \in I} \left(q_{jim} + N_{jim} \right)$. Constraints (23) specify the domain of the decision variables. We take the optimization results for fleet size $V_{max} = \sum_{i \in I} V_{i1}$ as the upper bound value for the number of vehicles required for the carsharing system.

Proposition 2. *The profit ϕ_{lb} obtained from **P2** is a lower bound to the optimal profit ϕ from **P1**.*
Proof. See Appendix.
Proposition 3. *Satisfying all demand and having vehicles fully charged before departure can provide the upper bound of the optimal fleet size in **P1**.*
Proof. See Appendix.

2) Fleet size lower bound V_{min}
To calculate a lower bound of the fleet size, we remove all the SOC related constraints (1)–(10) in **P1**. The optimization model is the following MILP

P3
$$\min_{\mathbf{S,V,Q,N}} \sum_{i \in I} V_{i1} \tag{24}$$

Subject to:

Constraints (13)–(18), plus

$$\phi_{lb} \le \sum_{t \in T} \sum_{i \in I} \sum_{j \in I} \left(c_0 - c_e \right) Q_{ijt} g_{ijt} - \sum_{i \in I} c_s S_i - \sum_{i \in I} c_f V_{i1} - \sum_{t \in T} \sum_{i \in I} \sum_{j \in I} c_r N_{ijt} g_{ijt} - \sum_{t \in T} \sum_{i \in I} \sum_{j \in I} c_p \left(q_{ijt} - Q_{ijt} \right) \tag{25}$$

The objective function (24) minimizes the vehicle fleet size. Constraints (25) require the total profit in **P3** to be larger than the minimum profit of **P1**. MILP **P3** aims to derive the minimum fleet size for obtaining a profit of at least ϕ_{lb}. Using EVs without battery capacity constraints indicates that the vehicles do not need to be recharged in carsharing operations. The cost parameters are the same as in **P1**.

Proposition 4. *Minimizing the fleet size by removing battery capacity constraints in the carsharing system can obtain the lower bound of the optimal fleet size in **P1**.*
Proof. See Appendix.

The optimization results in **P3** $V_{min} = \sum_{i \in I} V_{i1}$ are taken as the lower bound. The obtained station capacity $\{S_{min\ i}\}$ can serve as an initial value in the operational level problem.

3.2 Operational level decisions

Given a fleet size V_{sum} and station capacity $\{S_{min\ i}\}$, the operational level decides the satisfied travel demand Q_{ijt}, relocations N_{ijt}, and vehicle allocation V_{it}. A rolling horizon approach is developed to relax the non-linear constraints caused by the time-varying SOC of the vehicles. The operation decisions are divided into $|T|$ horizons. One horizon contains K time steps. Fig. 3 illustrates the rolling procedure. For example, the horizon t problem considers the optimization from time steps t to $t+K-1$. After the horizon t problem is solved, we roll to the next, horizon $t+1$ taking the optimization results before time instant $t+1$ as inputs (Berbeglia et al., 2010; Nielsen et al., 2012; Bertazzi and Maggioni, 2018; Liang et al., 2018).

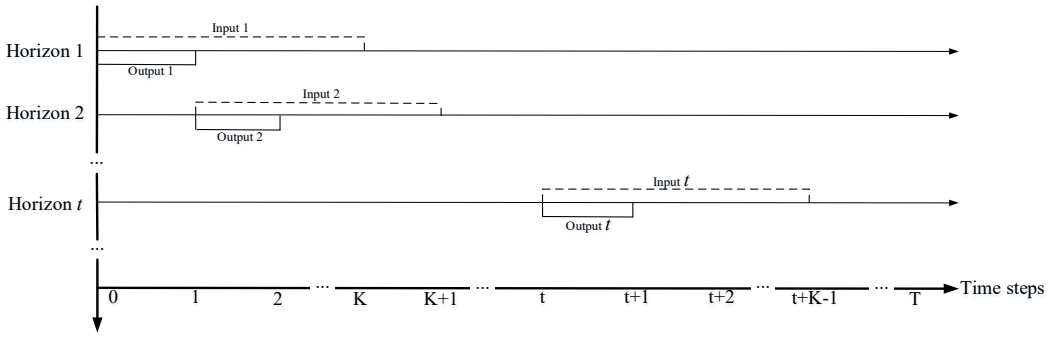

Fig. 3 Rolling horizon scheme

In the horizon t problem, the inputs include station capacity $\{S_{min\ i}\}$, available vehicles $V_{it}, \forall i \in I$ at time instant t, average SOC $\mu_{it}, \forall i \in I$ at time instant t, demand q_{ijk} and travel time g_{ijk} from time steps t to $t+K-1$, and all vehicle movements in previous time steps: Q_{ijm} and N_{ijm}, $\forall i, j \in I, m < t$. The aim of horizon t is to derive the optimized vehicle movements at time instant t (i.e., Q_{ijt}, N_{ijt}, $\forall i, j \in I$) such that the profits at time step t and the estimated profits at time steps $t+1$ to $t+K-1$ can be maximized.

The carsharing operational model at horizon t is formulated as the following LP model

P4-horizon-t

$$\max_{\mathbf{Q,N}} \sum_{i\in I}\sum_{j\in I}(c_0-c_e)Q_{ijt}g_{ijt} - \sum_{i\in I}\sum_{j\in I}c_r N_{ijt}g_{ijt} - \sum_{i\in I}\sum_{j\in I}c_p\left(q_{ijt}-Q_{ijt}\right) + \zeta\left(\sum_{k=t+1}^{t+K-1}\sum_{i\in I}\sum_{j\in I}(c_0-c_e)Q_{ijk}g_{ijk} - \sum_{k=t+1}^{t+K-1}\sum_{i\in I}\sum_{j\in I}c_r N_{ijk}g_{ijk} - \sum_{k=t+1}^{t+K-1}\sum_{i\in I}\sum_{j\in I}c_p\left(q_{ijk}-Q_{ijk}\right)\right) \tag{26}$$

Subject to:

$$\mu_{i1}=1 \quad \forall i\in I \tag{27}$$

$$\sum_{i\in I}V_{i1}=V_{sum} \tag{28}$$

$$Q_{ij_r t}+N_{ij_r t}\le V_{it}\left(1-F_{E_{it}}\left(\beta g_{ij_r t}\right)\right)-\sum_{n=r+1}^{|I|-1}\left(Q_{ij_n t}+N_{ij_n t}\right) \quad \forall i\in I,\ r\in 1,...,|I|-1 \tag{29}$$

$$V_{ik}\le S_i \quad \forall i\in I,\ k=t,...,t+K-1 \tag{30}$$

$$Q_{ijk}\le q_{ijk} \quad \forall i\in I,\ j\in I,\ k=t,...,t+K-1 \tag{31}$$

$$\sum_{j\in I}\left(Q_{ijk}+N_{ijk}\right)\le V_{ik} \quad \forall i\in I,\ k=t,...,t+K-1 \tag{32}$$

$$V_{ik+1}=V_{ik}-\sum_{j\in I}\left(Q_{ijk}+N_{ijk}\right)+\sum_{j\in I}\left(Q_{jim}+N_{jim}\right) \quad \forall i\in I,\ k=t,...t+K-2,\ m=max\left\{0,k+1-\left\lceil g_{jik}\right\rceil\right\} \tag{33}$$

$$N_{ijk},Q_{ijk}\ge 0,\ \forall i\in I,\ j\in I,\ k=t,...,t+K-1 \tag{34}$$

The objective function (26) maximizes the total profit for the operator from time steps t to $t+K-1$. We use ζ to weight the corresponding profits obtained from the estimated travel demand at time steps $t+1$ to $t+K-1$. Constraints (28) allocate the given number of vehicles V_{sum} to I traffic zones. Constraints (27) and (28) are required only for the first horizon. Constraints (30)–(34) capture the restrictions from time steps t to $t+K-1$ on parking space capacity, travel demand, vehicle movements, vehicle conservation over time, and the variable domain, respectively. V_{ik+1} is the number of shared EVs in zone i at time instant $k+1$. In Eq. (29), the limited EV battery capacity restricts vehicle movement at time instant t only. As the average SOC (μ_{it}) is known, its PDF $F_{E_{it}}\left(x\right)$ at time t is also known. Constraints (29) thus become linear. To circumvent the non-linear problem caused by the time-varying SOC of the vehicles, we eliminate the electricity conservation constraint when optimizing vehicle relocation from time steps $t+1$ to $t+K-1$. The LP **P4** can be readily solved using commercial solvers such as Gurobi, CPLEX (IBM), or Xpress (FICO).

By solving **P4**, we can obtain the satisfied travel demand Q_{ijt} and vehicle relocations N_{ijt} at time instant t, which are taken as outputs of horizon t. The next step is to calculate the average SOC μ_{it+1} at the next time instant $t+1$ using Eq. (10), and obtain available vehicles V_{it+1} using Eq. (33). These are used as inputs to the next horizon $t+1$. The process is repeated until all horizons $|T|$ are optimized.

The total profit, given a fleet size V_{sum} and station capacity $\{S_{min\,i}\}$ can thus be obtained as

$$\phi=\sum_{t\in T}\sum_{i\in I}\sum_{j\in I}(c_0-c_e)Q_{ijt}g_{ijt}-\sum_{i\in I}c_s S_i-\sum_{i\in I}c_f V_{i1}-\sum_{t\in T}\sum_{i\in I}\sum_{j\in I}c_r N_{ijt}g_{ijt}-\sum_{t\in T}\sum_{i\in I}\sum_{j\in I}c_p\left(q_{ijt}-Q_{ijt}\right) \tag{35}$$

where Q_{ijt} and N_{ijt} take their values from the corresponding horizon t.

The next step is to derive the optimized V_{sum} and $\{S_i\}$ to achieve a maximum total profit ϕ^*.

3.3 Shadow price and golden line search algorithm

We develop a shadow price algorithm to optimize the station capacity, and a golden section line search method to derive the optimized fleet size. The two searching routines iterate until the stopping criteria are satisfied.

We consider a given fleet size V_{sum} and derive the optimized $\{S_i\}$ first. In the rolling horizon framework, the dual value π_{it} to Constraints (30) provide information on the shadow price of the station capacity S_i. In other words, π_{it} indicates by how much the profit will increase if we have one more parking space $S_i + 1$. Adding up the shadow prices over all the time steps, the increase in the total profit by having one more parking space in traffic zone i is

$$\pi_i = \sum_{t \in T} \pi_{it} \tag{36}$$

If a profit increase of π_i is larger than the cost of renting parking space c_s, i.e., $\pi_i > c_s$, the number of parking spaces S_i in traffic zone i should increase in the next iteration

$$S_i := S_i + \delta \tag{37}$$

where δ is the number of added parking spaces. When π_i equals c_s, a near-optimal station capacity S_i is obtained (An and Lo, 2014; 2015).

The fleet size is optimized in the next step. We take the lower bound and upper bound of fleet size in **P2** and **P3** as the initial values and apply the golden section line search method to identify the near-optimal fleet size (Loxton et al., 2012). First, the lower bound and upper bound of fleet sizes are set as two boundary points. Second, two intermediate points are calculated based on the golden ratio: one is 0.618*(upper bound − lower bound) + lower bound, and another one is 0.382*(upper bound − lower bound) + lower bound. The corresponding profits at the two intermediate points are obtained by solving **P4**. Third, we find the intermediate point with the lower profit, and this is set as a new boundary point (upper bound or lower bound) to replace the original boundary point, whichever is closer. Finally, we repeat the second and third steps until meeting the stopping criteria: a small difference in profit between two boundary points.

The shadow price obtained in the rolling horizon framework helps with optimizing the strategic decisions on station capacity. At the operational level, both the satisfied travel demand Q_{ijt} and vehicle relocations N_{ijt} are relaxed to continuous variables. However, the optimization results show that only 0.01% of the variables Q_{ijt} and 13.42% of variables N_{ijt} take continuous values, based on the case study section. Furthermore, as most of Q_{ijt} and N_{ijt} take a value larger than 100, the continuous simplification has a marginal impact on the optimization results.

The following pseudo-code explains the proposed solution algorithm.

Step 1: Solve **P2** to get the fleet size V_{max}; solve **P3** to get the fleet size V_{min} and initial station capacity $\{S_{min\,i}\}$. The four golden section points are denoted by V_a, V_b, V_c, V_d where V_a, V_b are the two boundary points, and V_c, V_d are the intermediate points.

Step 2: Initialization. Set $V_a = V_{\min}$, $V_b = V_{\max}$, and $S_{ai} = S_i, S_{bi} = S_i$

Step 2.1: Given V_a and $\{S_{ai}\}$, solve **P4**, get the objective value ϕ_a. For the first iteration, $\phi_a^* = \phi_a$, otherwise, update the ϕ_a^* if $\phi_a^* \le \phi_a$.

Step 2.2: Calculate the marginal costs of π_{ai}.

Step 2.3: If $\pi_{ai} \le c_s$, go to Step 3; otherwise, set $S_{ai} := S_{ai} + \delta$ and go back to Step 2.1;

Step 3: Given V_b, S_{bi}, repeat Steps 2.1–2.3 to get the profits ϕ_b^*.

Step 4: Calculate $V_c = V_a + (1-\tau)(V_b - V_a)$, $V_d = V_a + \tau(V_b - V_a)$ where $\tau = (\sqrt{5}-1)/2$. Given V_c and V_d, repeat Steps 2.1–2.3 to get the profits ϕ_c^*, ϕ_d^*, respectively.

Step 5: If $V_b - V_a \le \varepsilon$, take $\phi^* = (\phi_c^* + \phi_d^*)/2$, $V^* = (V_c + V_d)/2$ and stop. Otherwise proceed to Step 6.

Step 6: If $\phi_c^* \ge \phi_d^*$, discard the segment $V_d \to V_b$, set $\phi_b^* = \phi_d^*$, $V_b = V_d$, $\phi_d^* = \phi_c^*$, $V_d = V_c$, go to Step 4; otherwise, discard the segment $V_a \to V_c$, set $\phi_a^* = \phi_c^*$, $V_a = V_c$, $\phi_c^* = \phi_d^*$, $V_c = V_d$, go to Step 4.

4 Application to the network at Suzhou Industrial Park

4.1 Setting up the case study

We implement the proposed electric carsharing optimization model at SIP in Suzhou, China. It contains 54 zones with a total area of 278 km^2, as shown in Fig. 4. The 54 zones are divided into three categories based on land use (residential zones: from zone #1 to zone #20, industrial zones: from zone #21 to #40, and commercial zones: from zone #41 to #50). Zones #51 to #54 correspond to undeveloped land with zero travel demand. According to the traffic census of 2017, 1.03 million citizens in the SIP region had generated 620 thousand trips per day by the end of 2016 (SIP, 2017). In this case study, those trips are taken as the potential carsharing travel demand. The upper bound of parking spaces is 5,000. We consider 13 hours of operation time in a typical working day for the electric carsharing system, from 7:00 to 20:00, which are further divided into 26 time steps with a duration of 30 minutes each. The distribution of the average departures per time step is constructed considering the time variation of trips and the land use features (Fig. 5). Given the average value, the actual travel demand to the other 49 zones from each zone is randomly generated following a uniform distribution between zero and two times the average value. The proposed model is solved using Python calling Gurobi 7.0.2 solver on a 3.40 GHz i7 processor, 28 GB RAM computer running the Windows 7 64-bit operating system.

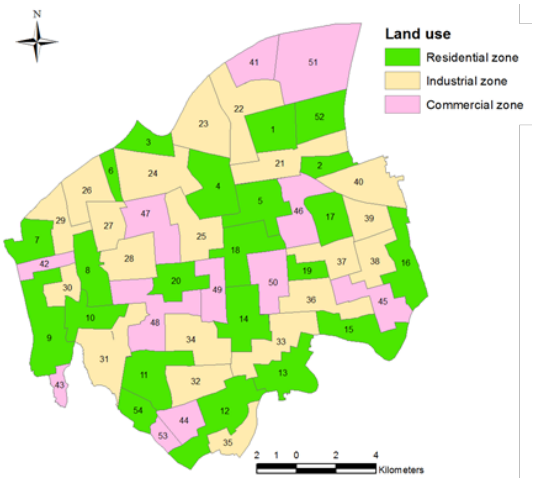

Fig. 4 Zoning of the SIP area

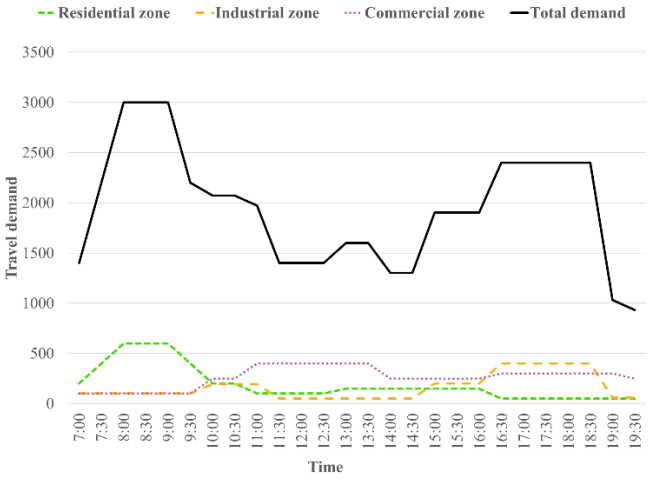

Fig. 5 Distribution of departures

The free-flow travel time of the shortest path is taken as the base travel time, which comes from the SIP road network as of 2012. The ArcGIS network analyst software is used to calculate the shortest distance between any two zone centroids. During a day, the traffic flow travel time is impacted by traffic congestion. Hence, the real-time traffic fluctuations are considered by setting growth factors for different time steps, as shown in Table 2.

Table 2 Growth factors of the travel time in relation to the shortest travel time

Time	7:00–7:59	8:00–9:59	10:00–10:59	11:00–11:59	12:00–13:59
Growth factor	1.0	1.5	1.3	1.1	1.2
Time	14:00–15:59	16:00–17:59	18:00–18:59	19:00–19:59	20:00–20:59
Growth factor	1.1	1.5	1.3	1.0	1.0

In this study, the parameters to be applied in the model are based on the operation of a one-way carsharing company (EVCARD) operating in China (http://www.evcard-sh.com) (Table 3).

Table 3 Parameters of the case study application

Parameter	c_0	c_e	c_r	c_f	c_s	c_p	K	α	β	ζ
Value	60	20	45	56	12	15	2	25	16.67	1
Unit	¥/h	¥/h	¥/h	¥/veh*day	¥/space*day	¥/trip	-	% per time step	% per time step	-

The rental price of a shared EV, c_0, the electricity consumption costs, c_e, vehicle fixed costs, c_f, vehicle relocation costs, c_r, and parking space rental costs, c_s, are taken from a previous research (Huang et al., 2018). The penalty for rejecting one trip is fixed at c_p = ¥15, which is taken as being the allowance for unserved clients to pay for a public transport ticket. K = 2 indicates that two time steps are looked at per horizon in the rolling horizon framework. The recharging speed α = 25% per time step indicates that vehicles can get fully charged in 4 time steps (2 hours). The discharging speed β is 16.67% per time step. The weight for the future profits, ζ, is considered to be 1, which indicates that the future profits have the same weight as the profits in the current time step. The SOC of the vehicles parked in traffic zone i at time step t obeys a uniform distribution based on the given average value

μ_{it} . At the operational level, we set the step size for the increase in station capacity (δ) as 100, and this is reduced to 10 in local searches, and we set the stopping criteria (ε) to be 500.

4.2 Optimization results

At the strategic level, the upper bound and lower bound of the fleet size obtained from **P2** and **P3** are 44,464 and 12,387, respectively. The two models are directly solved using Gurobi with computation times of 20 seconds and 162 seconds, respectively. The initial number of parking spaces obtained from **P3** is 42,064. At the operational level, the computation time is 3.93 hours using the proposed solution algorithm. Given a fleet size V_{sum} and station capacity $\{S_{min\ i}\}$, it takes an average of 3.89 seconds to solve the rolling horizon problem **P4** for one horizon, which adds up to 101 seconds to solve all the 26 horizons in a day to obtain the total profit. Given a fleet size V_{sum}, the shadow price algorithm iterates 10 times to identify the station capacity $\{S_i\}$ in 0.28 hours. On the outer circle (Fig. 2), in finding fleet size V_{sum}, the golden section method is executed 14 times with a total computation time of 3.93 hours. The optimization results show that the maximum profit is ￥4,488,400 ($718,144 at the current exchange rate) with a fleet size of 41,542 and 103,088 parking spaces. Fig. 6 illustrates the distribution of allocated vehicles and parking spaces in the SIP area. The numbers represent the fleet size at the beginning of a day, and the different shades of gray indicate station capacity. For daily operations, one vehicle services 11 trips a day, with an average driving time of 7.40 hours. Hence, the average vehicle usage rate is 56.92% during a 13-hour operation.

This case study considers an ideal carsharing market, and we consider all the trips in one typical workday in SIP as the potential carsharing demand. Travelers will choose carsharing if it is available and if no competition is considered. Thus, we investigate the performance of the electric carsharing system for the operator in a large-scale urban area. Currently, the market share of such systems is quite small compared with other modes of transport, such as private cars and public transport, owing to the price and convenience of the different competing modes of transportation.

Moreover, the operation costs in China may be lower than in other countries. For example, the costs of purchasing vehicles and renting parking spaces are low due to government subsidies promoting green travel in Suzhou. Consequently, the profit obtained in this case study may be quite high compared with operations in countries in Europe or operations in the United States. It is easy to adapt the proposed model and algorithm to any network given all the exogenous parameters.

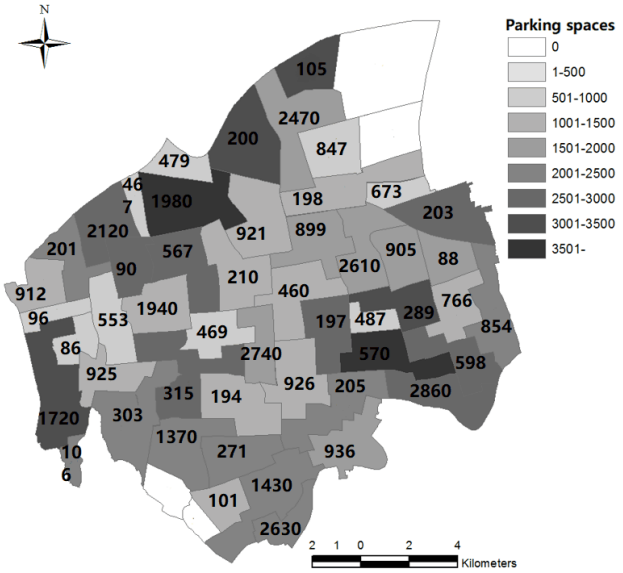

Fig. 6 Allocated vehicles and parking space distribution

4.2.1. Carsharing demand service ratio

We take the carsharing demand service ratio as a metric for measuring the effectiveness of the carsharing system. It is calculated as the ratio of satisfied demand to total demand. The results show that 77.12% of the demand is satisfied. We then further investigate the ratio in each zone at each time step (Fig. 7). Most of the values are above 60% for daily operations. In Fig. 7, low satisfied travel demand ratio occurs during the morning peak hours, noon, and afternoon peak hours. This happens owing to high travel demand being concentrated in short periods, which, in turn, means that the number of available vehicles is not sufficient to satisfy the demand for the service. Most notably, at 8:30 am and 9:00 am, the ratio in residential zones plummets to 40, which is caused by highly concentrated carsharing demand and limited available vehicles. There are only 9,191 parked vehicles attempting to service 21,907 carsharing requirements during this time step. Most vehicles parked in residential zones are rented at an early time during morning peak hours between 7:00 am and 8:30 am. However, they are relocated back in time, such that only 2,863 vehicles are relocated to the residential zones before 8:30 am. This causes significant vehicle shortage between 8:30 am and 9:00 am.

Fig. 7 Ratio of satisfied travel demand

The number of satisfied trip requests per trip duration are presented in Table 4. We divide the optimization results into 6 groups according to the trip duration $\leq$0.5, 0.5–1.0, 1.0–1.5, 1.5–2.0, 2.0–2.5, and $\geq$2.5 in time steps (where a time step has a duration of 30 minutes). Because vehicles use 16.67% electricity for driving during each time step, a fully charged vehicle can service a trip with a travel time of at most 6 time steps. In this selected case of SIP, the maximum travel distance is 2.85 time steps. The average patronage increases quickly with the increase of trip duration. It indicates that the operator can obtain larger profits when servicing long-duration trips.

Table 4 Ratio of satisfied demand for trips with different trip durations

Travel time	≤0.5	0.5–1.0	1.0–1.5	1.5–2.0	2.0–2.5	≥2.5
Average patronage	46.63%	73.06%	86.55%	89.69%	95.56%	100%

4.2.2. Vehicle relocations

Fig. 8 shows the number of relocated vehicles in the 50 traffic zones that constitute the urbanized region, indexed from 1 to 50. The ID of the traffic zones increases from left to right and from top to bottom. We selected 12 representative time steps in which the number of relocations is larger than 2,500. The

blue/green color denotes the vehicles relocated from/to the zone. A darker color indicates more vehicle relocations. The gray colors indicate that no relocation operation occurs from/to the zone.

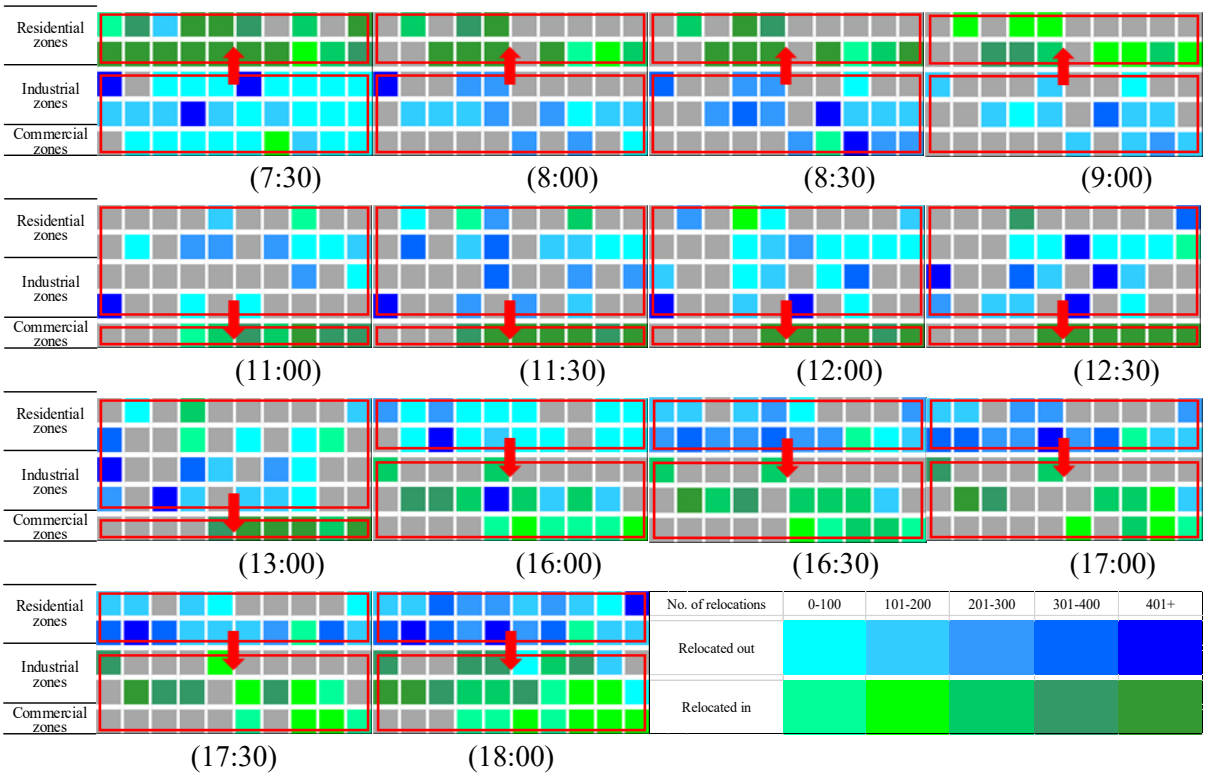

Fig. 8 Relocation operations

There are 54,469 relocations in this study area during an entire day of operation and they occur during three main periods: morning, noon, and afternoon peak hours. At the beginning of the day, citizens rent vehicles from home to the workplace, school, shopping center, etc. A large number of vehicles are relocated to the residential zones in the morning peak hours, from 7:30 to 9:29. The red arrow indicates the direction of vehicle relocations that come from industrial zones and commercial zones to residential zones. The travel demand in the commercial zones rises quickly at noon. Many vehicles are relocated to these zones from other zones in the period between 11:00 and 13:29. In the afternoon peak hours, from 16:00 to 18:29, many vehicles are relocated to both the industrial zones and commercial zones. Vehicle relocation operations are highly consistent with the three demand peaks shown in Fig. 5.

4.3 Sensitivity analysis

4.3.1 System performance under random demand

The rolling horizon framework can also handle random demand. As shown in Fig. 3, in a horizon, the satisfied travel demand is calculated based on the realized travel demand. The vehicle relocation operations are optimized based on the predictive travel demand.

To investigate the system performance under stochastic demand, we randomly generate 200 groups of travel requests. The carsharing requirements leaving one traffic zone per time step follows a normal distribution, in which the mean value is real departures in SIP and the coefficient of variation (CV) is 10%. CV is the ratio of standard deviation to the mean value. The fleet size and station capacity in the strategic level obtained from the baseline study are 41,542 vehicles and 103,088 parking spaces. The computation time was about 110 seconds for one demand scenario. Fig. 9 shows the optimization results.

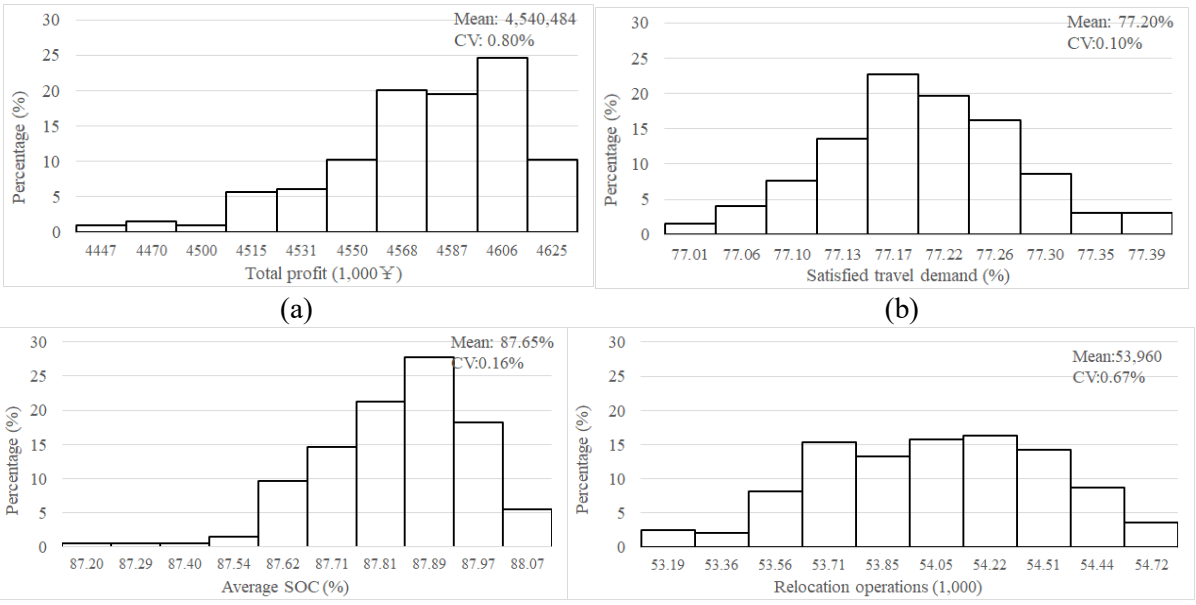

Fig. 9 Results under random demand, with a CV of 10%

We can see that the peak frequencies of the total profit (Fig. 9a), satisfied travel demand (Fig. 9b), average SOC (Fig. 9c), and the number of relocations (Fig. 9d) all happen around the mean values. The resultant CVs are as low as 0.80%, 0.10%, 0.16%, and 0.67%, respectively. Comparing to the base case, the average satisfied demand and the average SOC change marginally by +0.11% and −0.08%, respectively, whereas the average profit and average number of relocations change more significantly by +1.16% and −0.93%, respectively. Random demand seems to have a substantial impact on profit and vehicle relocation.

We further increase the CV to 30% and find that the distributions reported in Fig. 10 have higher variances and their peak frequencies still concentrate around the mean values. When increasing the CV of total demand to 30%, the CVs of total profits, satisfied travel demand, average SOC, and relocations increase to 1.32%, 0.26%, 0.28%, and 0.72%. Larger variations in demand (30%) yield only a relatively small fluctuation of the system performance metrics (0.28%, −1.32%).

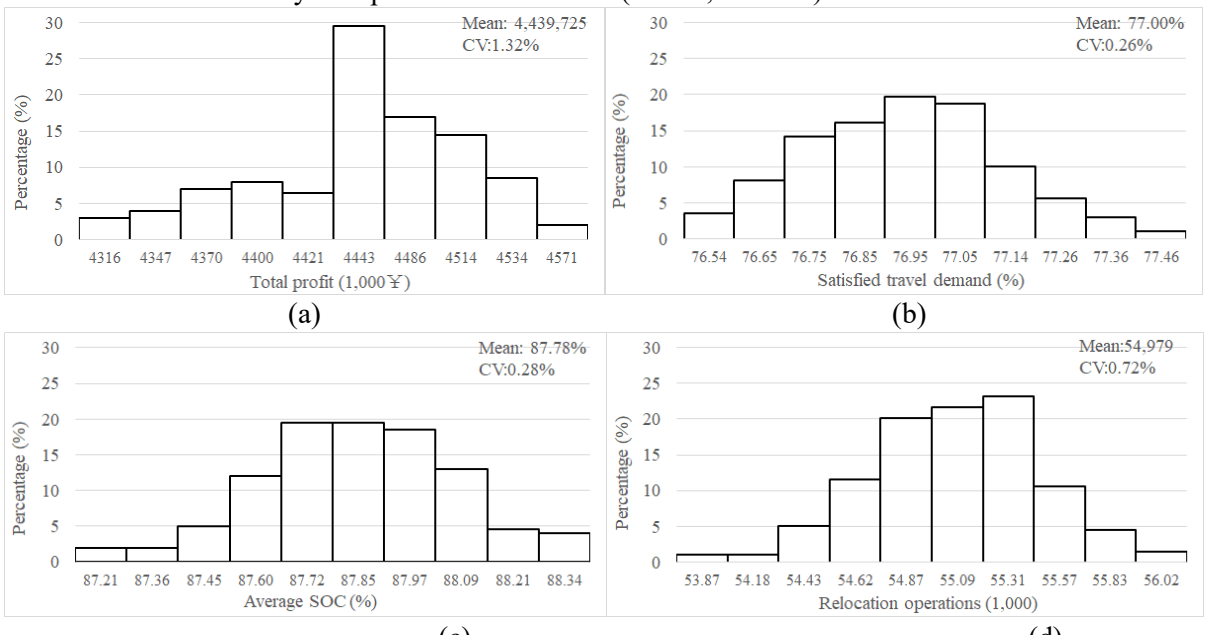

Fig. 10 Results under random demand, with a CV of 30%

4.3.2 System performance under various recharging speeds

This section analyzes the EV charging characteristics by setting different recharging speeds $\alpha =$ 50%, 25%, 16.67%, and 12.5% per time step, with a fixed discharging speed β of 16.67% per time step (one time step in this case study is 0.5 hour). The optimization results are presented in Table 5.

Table 5 Optimization results under different EV charging speeds

α (% per time step)	Profit (1000￥)	Fleet size	No. of parking spaces	Satisfied demand	Vehicle relocations	Average SOC
50	5,376	39,689	79,922	76.32%	70,490	95.81%
25	4,488	41,542	103,088	77.12%	54,469	87.72%
16.67	4,441	39,650	105,073	75.66%	52,399	71.89%
12.5	-855	31,785	89,982	37.24%	13,021	38.26%

In Table 5, the total profit drops substantially from ￥5,375,960 to ￥-855,307 when the charging speed decreases from 50% to 12.5% per time step. In practice, using slow chargers can significantly increase the vehicle charging time, thus lowering turnaround rates. This explains the decline in profits. At the same time, we find that the parking space-to-fleet size ratio increases, while the average SOC drops steeply. This happens because when charging speed is decreased, vehicles have to be parked for longer durations to be recharged. To provide carsharing service in a timely manner, more parking spaces are required. Furthermore, an interesting finding is that the allocated vehicles and satisfied travel requests do not continuously increase or decrease. When the recharging speed decreases from 50% to 25% per time step, both the fleet size and the percentage of satisfied demand drop. However, when the recharging speed decreases from 25% to 16.67% per time step, the fleet size increases, but the number of parking spaces decreases. This appears to suggest the need for the carsharing operator to weigh the costs of purchasing more vehicles against the demand loss penalty and the income generated by servicing more demand.

Furthermore, we find that vehicles have higher average SOC when faster charging speeds are considered. When fast chargers are used, it takes a shorter time for vehicles to recharge. Thus, they are able to obtain a sufficient battery capacity to service trip requests. Fig. 11 shows the average SOC over time. With a decrease in the charging speed, SOC fluctuates more drastically. The error bars in Fig. 11 show one standard deviation of the SOCs for the vehicles in the 53 traffic zones at each time step. We observe that the variance of the SOC also becomes larger when the charging speed decreases. When the charging speeds are lower than or equal to 12.5% per time step, we see an obvious decreasing trend in SOC over time, and the SOC cannot be recovered at the end of the daily operation after 13:00. In this study, we use the same installation price for different types of chargers although fast chargers are still more expensive. In practice, the operator can choose the most suitable charging technology to strike a proper balance between capital investment costs and market share.

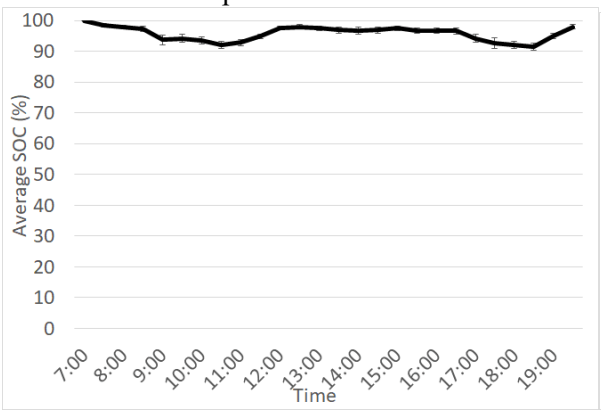

α = 50% per time step

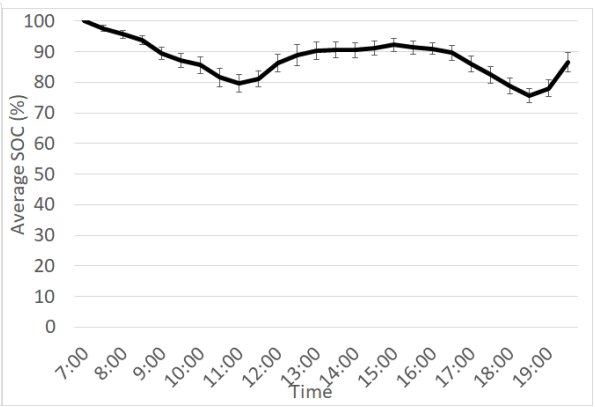

α = 25% per time step

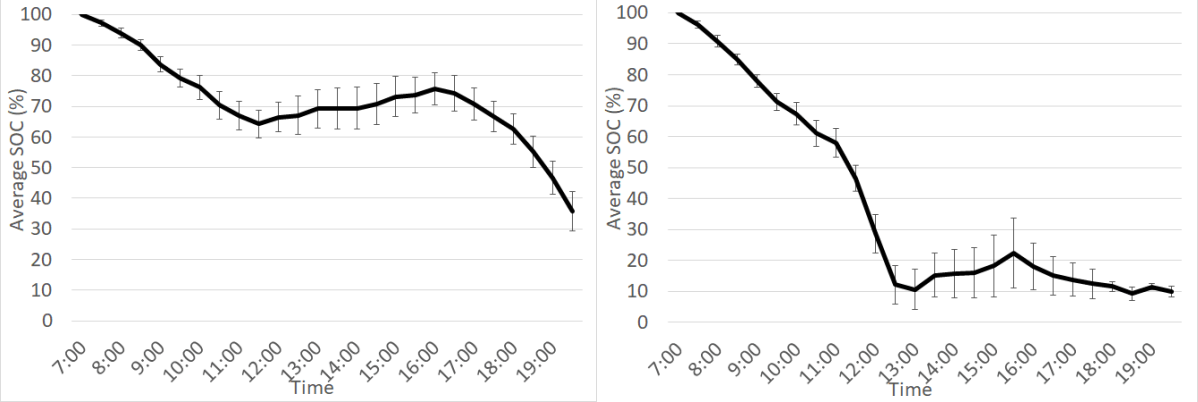

α = 16.67% per time step α = 12.5% per time step

Fig. 11 Average SOC and standard deviation

4.4 Verifying the continuous SOC distribution

An optimization model via tracking individual vehicle SOC and a discrete simulation model are proposed to figure out and verify the continuous SOC distribution. The optimization model applies to a small-scale traffic network while the simulation model verifies whether the uniform distribution is sensible in a large-scale traffic network.

4.4.1. Verification using an optimization model via tracking individual vehicle SOC

We built an optimization model **P5**. where the SOC of each vehicle can be traced (Gambella et al., 2018). We conducted a comparative analysis of the optimization results obtained by the original model **P1** (the continuous SOC distribution model) and the new model **P5**, which tracks the SOC of each vehicle. Considering the computation burden, we randomly chose a small number of zones (8, 10, or 13 zones) with 5 consecutive time steps in the SIP traffic network, and fix the fleet size. The original carsharing demand between OD pairs is used: 932, 1515, and 2,376 requirements in the selected 8 zones, 10 zones and 13 zones, respectively. Two different fleet sizes are provided in each traffic network: 250 and 300 in 8 zones, 400 and 450 in 10 zones, and 450 and 500 in 13 zones. Fast charge technology and slow charge technology are tested in each network. Combining these elements together, we construct 12 scenarios.

It is found that both the optimization results and SOC distributions are similar in the two models. Table 6 shows that the differences in profits, satisfied demand, and average SOC between the two models are lower than 3.2%, 5.0%, and 5.3%, respectively. In the two results, different groups of trips are satisfied, despite the percentage of satisfied trips being the same, which results in different profits. The two models are solved by different solution algorithms. Model **P5** is directedly solved using the Gurobi solver, which can be seen as the optimal results. For model **P1**, a rolling horizon is first used to simplify it by relaxing the non-linear constraints caused by the time-varying SOC of the vehicles. We calculate the difference in SOC for each vehicle obtained from model **P5** and the proposed model with a continuous SOC distribution. We find that about 65% of the SOC difference is within ±10% for the 10 scenarios. Especially in Scenarios 3, 4, 7, 8, 9, and 10, over 75% of the difference in SOC is within ±10%. This indicates that the continuous SOC distribution model can describe the battery capacity of vehicles parked at stations with a high level of accuracy. Hence, we believe that the proposed continuous SOC distribution model solved using the rolling horizon method is an effective method for reducing the computation burden, which aims to track the SOC of vehicles in groups without incurring a large error with such simplification.

Table 6 Differences between two optimization models

Scenario	No. of zones	Total demand	Fleet size	Charging/Discharging speed (% per time step)	Model **P1** (Continuous SOC distribution)				Model **P5** (tracking individual vehicle SOC)			
					Profits	Satisfied demand (%)	Average SOC (%)	Computation time (s)	Profits (%)	Satisfied demand (%)	Average SOC (%)	Computation time (s)
1	8	932	250	25/33	45,665	93.03	94.12	8	+1.1	0	+0.8	361
2	8	932	300	25/33	46,602	98.50	95.35	7	+1.1	0	+0.6	415
3	8	932	250	13/66	44,832	88.95	68.33	11	+3.2	+4.6	+1.9	2,137
4	8	932	300	13/66	46,207	95.06	73.26	11	+2.0	+3.6	+3.1	2,968
5	10	1,514	400	25/33	75,308	91.74	93.90	8	+0.9	−0.2	+0.6	2,896
6	10	1,514	450	25/33	76,427	96.30	94.70	8	+0.9	0	+0.7	3,224
7	10	1,514	400	13/66	73,984	87.22	64.36	14	+2.7	+5.0	+5.1	49,227
8	10	1,514	450	13/66	75,873	94.78	68.02	13	+1.5	1.5	+5.3	13,828
9	13	2,376	450	25/33	101,495	81.73	92.68	8	+0.9	0	+0.3	12,631
10	13	2,376	500	25/33	104,982	86.53	93.61	8	+0.9	−0.4	+0.4	20,202
11	13	2,376	450	13/66	--	--	--	13	--	--	--	--
12	13	2,376	500	13/66	--	--	--	13	--	--	--	--

4.4.2. Verification by discrete event simulation

A discrete event simulation model was developed to analyze the distribution of the SOC of vehicles parked at a station, and to check the assumption of a continuous uniform SOC distribution. We use the fleet size, station capacity, and vehicle movements from the optimization results of our proposed models as input for the simulation. The inconsistent vehicle movements are all recorded. For example, 10 vehicles are supposed to move from zone A to zone B. However, only 8 vehicles have enough SOC to do so. Thus, the other 2 vehicles will be retained in zone A. Three simulations are performed: Case 1 with the base case, Case 2 with low charging speed ($\alpha =$ 12.5%), and Case 3 with a low travel demand ratio of 20%.

For a better understanding of the SOC distribution, Fig. 12 shows the difference in vehicle SOC between our proposed continuous SOC distribution model **P1** and the discrete simulation. The horizontal axis represents the difference between the SOC of each vehicle in the 50 zones at 26 time steps in the proposed model **P1,** and the SOC in the discrete simulation. The vertical axis indicates the proportion of each group. In all the three cases, we can see that over 70% of the vehicles are within the range of ±5% of SOC difference and over 80% vehicles are within ±10%. This indicates that the continuous SOC distribution model can describe the battery capacity of vehicles parked at stations with a relatively high level of realism. In this study, the assumption of a uniform distribution is therefore regarded as acceptable.

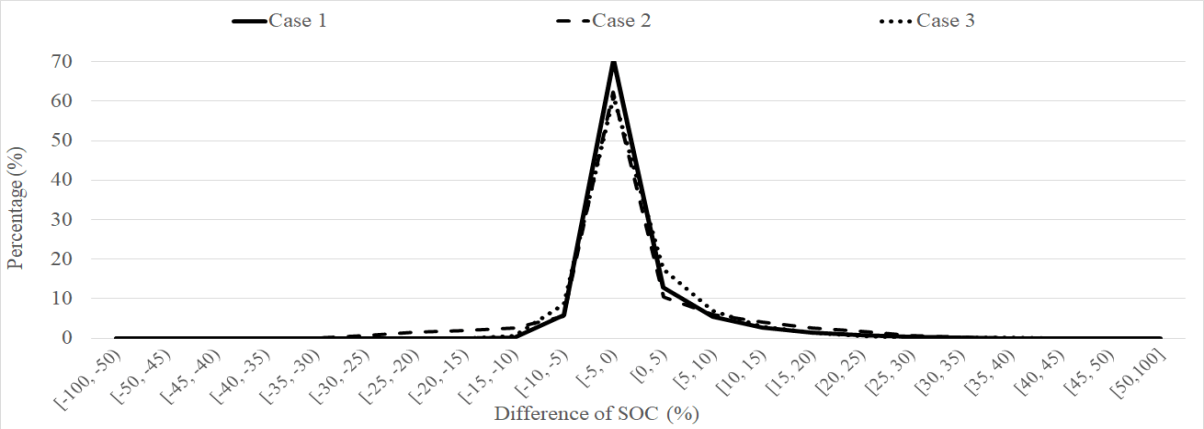

Fig. 12 Difference in SOC between the continuous SOC distribution and the discrete simulation results

4.4.3. Further improvement of the continuous SOC distribution model

In the cases that failed the uniform distribution test, we found that most had an extremely high percentage of vehicles having a SOC larger than 95%. We also observed that these exceptions only occur when the average SOC is larger than 90%. To verify this, in Fig. 13, we plot the percentage of vehicles with the highest SOC range against the average SOC in this station. The highest SOC range is calculated as follows: the SOC is divided into ranges with a size of 5%. If the vehicles at a station have an SOC from 50%–82%, the highest SOC range would be 77%–82%. Fig. 13 shows that when the average SOC is over 90%, the percentage of vehicles with extremely high SOC increases significantly with the increase in average SOC. This demonstrates that the exception occurs only when the average SOC is relatively high. Regardless of these exceptions, the overall performance of the proposed model is acceptable when compared with the discrete simulation results, as seen in Fig. 12.

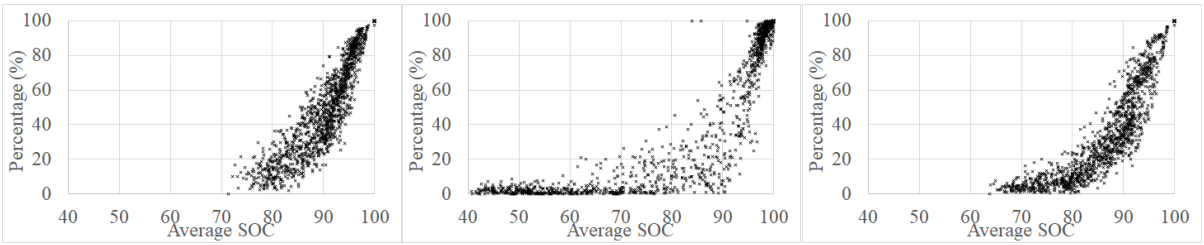

Fig. 13 Distribution of the percentage of vehicles in the last SOC

To rectify such errors, we amend the SOC distribution when the average SOC is larger than 90% by separating the continuous SOC distribution model into two parts. One part follows a uniform distribution (UD1) with mean μ_{it}^{upper}, and the second part follows another uniform distribution (UD2) with mean μ_{it}^{lower}. Let $\mu_{it}^{upper} = \left(\mu_{it} + 100\%\right)/2$, where μ_{it} is the average SOC of vehicles in zone i at time instant *t*. The revised continuous SOC distribution model is designed such that 60% of the vehicles belong to UD1 when the average SOC is higher than 90%. The metrics for measuring the exceptions (average SOC larger than 90%, 60% of vehicles belong to UD1) are obtained from the statistics in Fig. 13, and are applied only in this case study. Table 7 presents the optimization and simulation results before and after these changes.

Table 7 Optimization and simulation results

Scenario	Optimization /simulation	Profit (1000￥)	Penalty (1000￥)	Satisfied demand	Vehicle relocations	Average SOC	Computation time (h)
Before	Optimization	4,488	647	77.1%	54,469	87.72%	3.93
	Simulation	3,855	822	72.4%	53,321	91.06%	4.78
After	Optimization	4,651	590	78.7%	54,114	85.53%	4.05
	Simulation	4,019	764	74.1%	52,718	91.40%	4.70

Before the changes, considering the SOC difference, the simulation method cannot ensure that all the vehicle movements from the optimization are performed. The proportion of satisfied demand dropped from 77.1% to 72.4% (4.7% difference) in the simulation, and 5.54% vehicle movements (either for demand satisfaction or relocation) cannot be performed in the simulation. Consequently, the profit also drops 14.10%. The reason is that the uniform distribution in the SOC estimation is not compatible with some trips in the simulation. When rolling 26 time steps, the error gradually accumulates over time. Hence, the satisfied demand and profit are low and the penalty apparently high in the simulation model.

After the changes are applied to the model, the proportion of satisfied demand dropped from 78.7% to 74.1% (4.6% difference) in the simulation, and 5.52% of vehicle movements cannot be carried out in the simulation. The profit also drops 13.61%. The number of available vehicles in the simulation is closer to the optimization due to the lower error in the SOC estimation, which is shown in Fig. 14b. We can see that the profits and satisfied demand become larger, and the differences in the profits and vehicle movements are smaller. However, the average SOC in the optimization model decreases to 85.53% after these changes. These results indicate that separating the SOC distribution into two parts has marginal impact on the results.

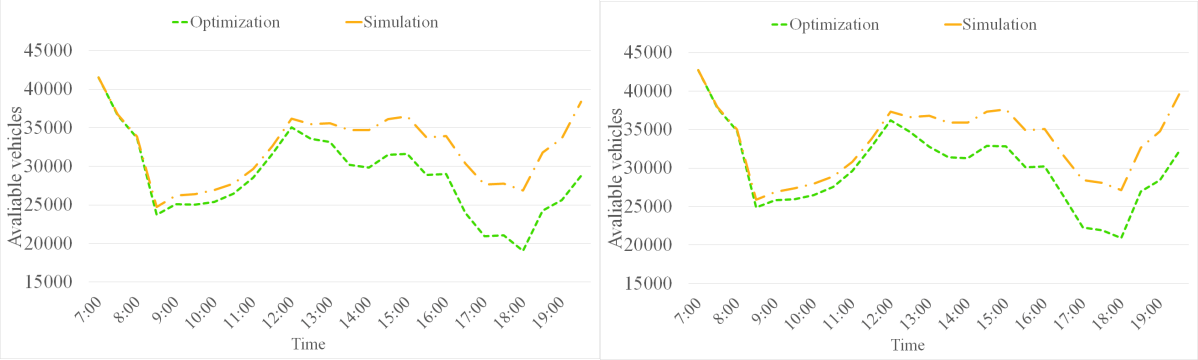

a. Before the changes b. After the changes

Fig. 14 Available vehicles $\sum_{i\in I} V_{it}$ over time

Here, we present only one possible way to further improve the approximation accuracy of the SOC model. Because its small impact in this case study, we decided to use the original model with no SOC distribution changes in all the analyses.

4.5 Remarks on the continuous SOC distribution and solution methods

The goal of this study is to determine the station capacity and fleet size of a one-way carsharing system using EVs. Considering the non-linear problems in the MINLP, the SOC distribution and solution algorithms, including the rolling horizon framework and shadow price, are introduced at the operational decision level. Those relaxations make this model solvable. A near-optimal solution can be obtained for the entire problem. Moreover, the small differences between the two optimization models, tracking the SOC of each vehicle, and the continuous SOC distribution, also indicate that using a rolling horizon to relax the non-linear integral functions delivers high-quality solutions. The average differences are 1.50%, 1.50%, and 1.82% of profits, satisfied demand, and average SOC, respectively. In this study, the satisfied travel demand is determined by maximizing the profits yielded at the current time step. The number of relocations is determined by maximizing the estimated profits generated at future time steps. Thus, different horizons are connected through the vehicle relocations.

As shown in Table 6, when the fleet size is larger than 500, we could not obtain results in 24 hours in Scenario 11 and Scenario 12. Therefore, the method of tracking the SOC of each vehicle is only applicable when the fleet size is very small. However, studies show that carsharing companies are expanding rapidly. For example, EVCARD, the largest one-way carsharing company in China, had 1,739 parking stations and over 5,000 vehicles as of March 2017, in Shanghai, China alone (Wang et al., 2019). The number of parking stations owned by EVCARD have increased to more than 3,600 in two years. It is very challenging for the exact optimization model with individual vehicle tracking to handle those existing 5,000 vehicles. Therefore, the proposed method in this study enables us to handle a relatively large network with over 5,000 vehicles.

We can only ensure the local optimum of the results obtained via the golden section line search in this study. Because there is no strict limit on the computation time for the strategic level problem, we can also use a heuristic search algorithm to find a better solution. For example, we can adopt an enumeration algorithm with a step size of 500. When there are 65 iterations, we find that the largest profit happens at the fleet size of 41,500, which is close to the optimal fleet size derived in our study. A smaller step size can be used to enhance the solution quality further, although at the expense of longer computation time.

5 Conclusion

This study proposes an MINLP model for maximization the profit of a station-based one-way electric carsharing system operator by determining the EV fleet size and station capacity. To solve the computation challenges caused by demand fluctuations and the time-varying SOC of the vehicles, we divide the MINLP model into two subproblems: one for the strategic level and the other for the operational level. The station capacity and fleet size are optimized in the strategic level problem via a shadow price and the golden section line search method, which are taken as inputs to the operational level problem. The operational decisions are optimized using a rolling horizon framework. A practical case consisting of 54 traffic zones for 13 hours of operation with 26 time steps is constructed to demonstrate the efficiency of the proposed model and algorithm.

The optimization results show that a maximum total profit of ￥4,488,400 ($718,144) is obtained when the rate of satisfied demand reaches 77.12%. The fleet size and station capacity are optimized after 140 iterations with 3.93 hours computation time, which cannot be obtained in 24 hours when tracking the individual vehicle SOC. Using the proposed continuous SOC distribution model rather than tracking every EV simplifies the MINLP model and relieves the heavy computation burden. The results from an optimization model via tracking individual vehicle SOC and a discrete event simulation demonstrate that the SOC model can adequately capture the SOC distribution of vehicles at a station. Charging speeds have significant impact on vehicle turnaround rates. Using fast charging technology, the operator can obtain large profits by cutting operation costs and increasing service rate. Thus, the operator has to weigh the opportunity for increased carsharing service income against the costs of vehicle purchase.

This study can be improved in the following ways: This study assumes that a parking space should be installed with a charging pile. This, however, may result in resource waste because not all parked vehicles require charging. Optimizing the number of charging piles needed in a parking station is a relevant challenge for the one-way carsharing system. Furthermore, the problem of considering stochastic travel demand is very challenging. In this study, the demand for carsharing is fixed and given. However, in reality, carsharing competes with other travel modes whose shares are typically estimated using discrete choice models. The travel mode of choice is eventually decided by the users' utility functions. Carsharing pricing is an effective tool for encouraging potential users or reducing their enthusiasm (Angelopoulos et al., 2018). Finding an appropriate pricing strategy that strikes a balance between demand and vehicle supply is another possible extension.

References

An, K., & Lo, H. K. (2014). Ferry service network design with stochastic demand under user equilibrium flows. Transportation Research Part B, 66(8), 70-89.

An, K., & Lo, H. K. (2015). Robust transit network design with stochastic demand considering development density. Transportation Research Part B, 81, 737-754.

Angelopoulos, A., Gavalas, D., Konstantopoulos, C., Kypriadis, D., & Pantziou, G. (2018). Incentivized vehicle relocation in vehicle sharing systems. Transportation Research Part C, 97, 175-193.

Berbeglia, G., Cordeau, J. F., & Laporte, G. (2010). Dynamic pickup and delivery problems. European journal of operational research, 202(1), 8-15.

Bertazzi, L., & Maggioni, F. (2018). A stochastic multi-stage fixed charge transportation problem: Worst-case analysis of the rolling horizon approach. European Journal of Operational Research, 267(2), 555-569.

Boyacı, B., Zografos, K. G., & Geroliminis, N. (2017). An integrated optimization-simulation framework for vehicle and personnel relocations of electric carsharing systems with reservations. Transportation Research Part B, 95, 214-237.

Brandstätter, G., Kahr, M., Leitner, M., & Mannering, F. (2017). Determining optimal locations for charging stations of electric car-sharing systems under stochastic demand. Transportation Research Part B, 104, 17-35.

Bruglieri, M., Pezzella, F., & Pisacane, O. (2017). Heuristic algorithms for the operator-based relocation problem in one-way electric carsharing systems. Discrete Optimization, 23, 56-80.

Cepolina, E. M., & Farina, A. (2012). A new shared vehicle system for urban areas. Transportation Research Part C, 21(1), 230-243.

Correia, G., & Santos, R. (2014). Optimizing the use of electric vehicles in a regional car rental fleet. Transportation Research Record: Journal of the Transportation Research Board, (2454), 76-83.

Correia, G., & Antunes, A. P. (2012). Optimization approach to depot location and trip selection in one-way carsharing systems. Transportation Research Part E, 48(1), 233-247.

Deng, Y., & Cardin, M. A. (2018). Integrating operational decisions into the planning of one-way vehicle-sharing systems under uncertainty. Transportation Research Part C, 86, 407-424.

Fassi, A. E., Viviani, M., & Viviani, M. (2012). Evaluation of carsharing network's growth strategies through discrete event simulation. Pergamon Press, Inc, 39(8): 6692-6705.

Firnkorn, J., & Müller, M. (2015). Free-floating electric carsharing-fleets in smart cities: the dawning of a post-private car era in urban environments? Environmental Science & Policy, 45, 30-40.

Gambella, C., Malaguti, E., Masini, F., & Vigo, D. (2018). Optimizing relocation operations in electric car-sharing. Omega.

Hu, L., & Liu, Y. (2016). Joint design of parking capacities and fleet size for one-way station-based carsharing systems with road congestion constraints. Transportation Research Part B, 93, 268-299.

Hua, Y., Zhao, D., Wang, X., & Li, X. (2019). Joint infrastructure planning and fleet management for one-way electric car sharing under time-varying uncertain demand. Transportation Research Part B, 128, 185-206.

Huang, K., de Almeida Correia, G. H., & An, K. (2018). Solving the station-based one-way carsharing network planning problem with relocations and non-linear demand. Transportation Research Part C, 90, 1-17.

Jorge, D., Barnhart, C., & de Almeida Correia, G.. (2015). Assessing the viability of enabling a round-trip carsharing system to accept one-way trips: Application to Logan Airport in Boston. Transportation Research Part C, 56, 359-372.

Jorge, D., Correia, G., & Barnhart, C. (2012). Testing the validity of the mip approach for locating carsharing stations in one-way systems. Procedia - Social and Behavioral Sciences, 54, 138-148.

Jorge, D., Correia, G., & Barnhart, C. (2014). Comparing optimal relocation operations with simulated relocation policies in one-way carsharing systems. IEEE Transactions on Intelligent Transportation Systems, 15(4), 1667-1675.

Jung, J., & Koo, Y. (2018). Analyzing the Effects of Car Sharing Services on the Reduction of Greenhouse Gas (GHG) Emissions. Sustainability, 10(2), 539.

Kek, A. G., Cheu, R. L., Meng, Q., & Fung, C. H. (2009). A decision support system for vehicle relocation operations in carsharing systems. Transportation Research Part E, 45(1), 149-158.

Li, X., Ma, J., Cui, J., Ghiasi, A., & Zhou, F. (2016). Design framework of large-scale one-way electric vehicle sharing systems: a continuum approximation model. Transportation Research Part B, 88, 21-45.

Liang, X., Correia, G., & Bart, A. (2016). Optimizing the service area and trip selection of an electric automated taxi system used for the last mile of train trips. Transportation Research Part E, 93, 115-129.

Liang, X., Correia, G., & Bart, A. (2018). Applying a model for trip assignment and dynamic routing of automated taxis with congestion: system performance in the city of Delft, The Netherlands. Transportation Research Record Journal of the Transportation Research Board.

Loxton, R., Lin, Q., & Teo, K. L. (2012). A stochastic fleet composition problem. Computers & Operations Research, 39(12), 3177-3184.

Lu, C. C., Yan, S., & Huang, Y. W. (2018). Optimal scheduling of a taxi fleet with mixed electric and gasoline vehicles to service advance reservations. Transportation Research Part C, 93, 479-500.

Nair, R., & Miller-Hooks, E. (2014). Equilibrium network design of shared-vehicle systems. European Journal of Operational Research, 235(1), 47-61.

Nielsen, L. K., Kroon, L., & Maróti, G. (2012). A rolling horizon approach for disruption management of railway rolling stock. European Journal of Operational Research, 220(2), 496-509.

Scheltes, A., & Correia, G. (2017). Exploring the use of automated vehicles as last mile connection of train trips through an agent-based simulation model: An application to Delft, Netherlands. International Journal of Transportation Science and Technology, 6(1), 28-41.

Shaheen, S. A., Chan, N. D., & Micheaux, H. (2015). One-way carsharing's evolution and operator perspectives from the americas. Transportation, 42(3), 519-536.

SIP., 2017. <http://www.sipac.gov.cn/dept/wtjd/xwzx/201701/t20170119_524571.htm> (accessed: 2019-7-29).

Wang, L., Liu, Q., & Ma, W. (2019). Optimization of dynamic relocation operations for one-way electric carsharing systems. Transportation Research Part C, 101, 55-69.

Xu, M., Meng, Q., & Liu, Z. (2018). Electric vehicle fleet size and trip pricing for one-way carsharing services considering vehicle relocation and personnel assignment. Transportation Research Part B, 111, 60-82.

Yang, J., Dong, J., Lin, Z., & Hu, L. (2016). Predicting market potential and environmental benefits of deploying electric taxis in Nanjing, China. Transportation Research Part D, 49, 68-81.

Yoon, T., Cherry, C. R., & Jones, L. R. (2017). One-way and round-trip carsharing: A stated preference experiment in Beijing. Transportation research part D, 53, 102-114.

Zhang, D., Liu, Y., & He, S. (2019). Vehicle assignment and relays for one-way electric car-sharing systems. Transportation Research Part B, 120, 125-146.

Zhao, M., Li, X., Yin, J., Cui, J., Yang, L., & An, S. (2018). An integrated framework for electric vehicle rebalancing and staff relocation in one-way carsharing systems: Model formulation and Lagrangian relaxation-based solution approach. Transportation Research Part B, 117, 542-572.